Comput Mech (2008) 42:305–315
DOI 10.1007/s00466-007-0213-7

ORIGINAL PAPER

Adaptive multi-analysis strategy for contact problems with friction

Application to aerospace bolted joints

L. Champaney · P.-A. Boucard · S. Guinard

Received: 28 November 2006 / Accepted: 21 July 2007 / Published online: 29 August 2007

Abstract The objective of the work presented here is to develop an efficient strategy for the parametric analysis of bolted joints designed for aerospace applications. These joints are used in elastic structural assemblies with local nonlinearities (such as unilateral contact with friction) under quasi-static loading. Our approach is based on a decomposition of an assembly into substructures (representing the parts) and interfaces (representing the connections). The problem within each substructure is solved by the finite element method, while an iterative scheme based on the LATIN method (Ladevèze in Nonlinear computational structural mechanics—new approaches and non-incremental methods of calculation, 1999) is used for the global resolution. The proposed strategy consists in calculating response surfaces (Rajashekhar and Ellingwood in Struct Saf 12:205–220, 1993) such that each point of a surface is associated with a design configuration. Each design configuration corresponds to a set of values of all the variable parameters (friction coefficients, prestresses) which are introduced into the mechanical analysis. Here, instead of carrying out a full calculation for each point of the surface, we propose to use the capabilities of the LATIN method and reutilize the solution of one problem (for one set of parameters) in order to solve similar problems (for the other sets of parameters) (Boucard and Champaney in Int J Numer Methods Eng 57:1259–1281, 2003). The strategy is adaptive in the sense that it takes into account the results of the previous calculations. The method presented can be used for several types of nonlinear problems requiring multiple analyses: for example, it has already been used for structural identification (Allix and Vidal in Comput Methods Appl Mech Eng 191:2727–2758, 2001).

Keywords Parametric uncertainties · Contact · Friction · Nonincremental method · Substructuring method

L. Champaney · P.-A. Boucard (✉)
LMT-Cachan, (ENS Cachan/CNRS/Universite
Paris 6/UniverSud Paris), 61 av. du President Wilson,
94230 Cachan, France
e-mail: boucard@lmt.ens-cachan.fr

S. Guinard
EADS-IW, 18, rue Marius Terce-BP 13050,
31025 Toulouse Cedex 03, France
e-mail: stephane.guinard@eads.net

1 Introduction

The resolution of deterministic problems is often carried out using finite element analysis (FEA). For structural engineers, the incorporation of a system's parametric uncertainties into such an analysis constitutes a challenge; however, without this information, the structural response cannot be calculated accurately. These parametric uncertainties may affect the material's mechanical properties (modulus, strength, etc.), the structure's geometric properties (cross-sectional properties and dimensions), the boundary conditions (including contact with friction), the magnitude and distribution of loads, etc. In the case of structural assemblies, the knowledge of the friction coefficients is especially limited. In order to take these uncertainties into account, it is necessary to calculate the response of the structure for each set of values of the design parameters [5]. Typically, in our case, the design parameters are the friction coefficients and the prestresses in some bolts.

The objective of the work presented here is to develop a strategy which is suitable for problems involving multiple resolutions. Therefore, the choice of an accurate and efficient computational method is of vital importance. Our approach is based on a decomposition of an assembly into substructures

and interfaces. The interfaces represent the different types of connections. They play the vital role of enabling local nonlinearities, such as contact and friction, to be modeled easily and accurately. The problem within each substructure is solved by the finite element method, while an iterative scheme based on the LATIN method is used for the global resolution. More specifically, the objective pursued is to calculate a large number of design configurations, each corresponding to a set of values of all the variable parameters (friction coefficients, prestresses) involved in the mechanical analysis. A full calculation is normally needed for each set of parameters. Here, as an alternative, we propose to take advantage of the capabilities of the LATIN method and reuse the solution of one problem (for one set of parameters) to solve similar problems (for the other sets of parameters).

The numerical examples presented deal with 3D applications, one of them being an aerospace bolted joint. For some of these examples, over a thousand different calculations had to be carried out for the parametric study. The comparison with classical industrial codes in terms of computation costs shows that our algorithm is very efficient.

2 The LATIN method

Here, we will review only the main aspects of the LATIN method. The details of the method itself can be found in [1] and those of its particular application to computational contact problems in [6,7].

2.1 Decomposition of an assembly

An assembly is composed of a set of *substructures* (each substructure is a component of the assembly) which communicate with one another through *interfaces* (each interface represents a connection), see Fig. 1. Each interface is a mechanical entity with its own variables and its specific behavior, which depends on the type of connection. Many different connection types can be modeled by this approach, but in this paper we consider only classical contact connections. Two connected substructures are denoted Ω_E and $\Omega_{E'}$ and the associated interface is designated by $\Gamma^{EE'}$.

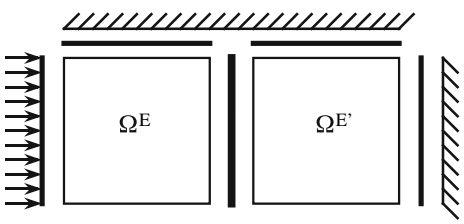

Fig. 1 Decomposition of an assembly

Fig. 2 Interface variables

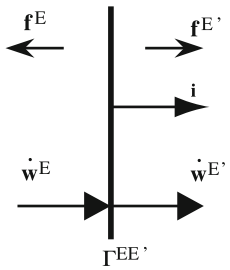

The interface variables are two force fields $\mathbf{f}^E$ and $\mathbf{f}^{E'}$ and two dual velocity fields $\dot{\mathbf{w}}^E$ et $\dot{\mathbf{w}}^{E'}$ (Fig. 2). By convention, $\mathbf{f}^E$ and $\mathbf{f}^{E'}$ are the actions of the interface on the substructures and $\dot{\mathbf{w}}^E$ et $\dot{\mathbf{w}}^{E'}$ are the velocities of the substructures seen from the interface.

2.2 The problem in the substructures

The displacement field at any point M of Ω_E and at any time t of $[0, T]$ is $\mathbf{u}^E(M, t)$; the associated space is $\mathscr{U}^{[0,T]}$. ϵ is the strain field and the current state of the structure is characterized by the stress field σ^E.

The mechanical problem to be solved in *each substructure* is:

Find the histories of the displacement field $\mathbf{u}^E(M, t)$ and stress field $\sigma^E(M, t)$ such that:

– Kinematic admissibility: $\forall M \in \Omega_E$, $\forall t \in [0, T]$,

$$\epsilon = \epsilon(\mathbf{u}^E); \quad \mathbf{u}^E \in \mathscr{U}^{[0,T]}$$
$$\dot{\mathbf{u}}^E(M, t)_{|\partial\Omega_E} = \dot{\mathbf{w}}^E(M, t) \tag{1}$$

– Equilibrium: $\forall \dot{\mathbf{u}}^\star \in \mathscr{U}_0^{[0,T]}$ $\forall M \in \Omega_E$, $\forall t \in [0, T]$,

$$\int_{\Omega_E} Tr(\sigma^E \epsilon(\dot{\mathbf{u}}^\star))\mathrm{d}\Omega_E - \int_{\partial\Omega_E} \mathbf{f}^E.\dot{\mathbf{u}}^\star \mathrm{d}S = 0 \tag{2}$$

where $\mathscr{U}_0^{[0,T]}$ is the set of finite-energy velocity fields on Ω_E which vanish on $\partial\Omega_E$ and $\dot{\mathbf{u}}^\star$ a virtual velocity field. We assume that there are no body forces in Ω_E.

– Elastic behavior: $\forall M \in \Omega_E$, $\forall t \in [0, T]$,

$$\sigma^E(M, t) = \mathbf{D}\epsilon(\mathbf{u}^E(M, t)) \tag{3}$$

where $\mathbf{D}$ is Hooke's operator.

2.3 The problem on the interfaces

The mechanical problem to be solved on each interface is

Find the histories of the force fields ($\mathbf{f}^E(M, t)$ and $\mathbf{f}^{E'}(M, t)$) and of the velocity fields ($\dot{\mathbf{w}}^E(M, t)$ and $\dot{\mathbf{w}}^{E'}(M, t)$) such that:

– Equilibrium: $\forall M \in \Gamma^{EE'}$ and $\forall t \in [0, T]$,

$$\mathbf{f}^E(M,t) + \mathbf{f}^{E'}(M,t) = 0 \tag{4}$$

– Behavior: $\forall M \in \Gamma^{EE'}$ and $\forall t \in [0, T]$,

$$\mathbf{f}^E(M,t) = \mathscr{R}(\dot{\mathbf{w}}^{EE'}(M,\tau), \tau \in [0,t]) \tag{5}$$

where the behavior is expressed as a nonlinear evolution law $\mathscr{R}$ between the forces and the rate $\dot{\mathbf{w}}^{EE'}$ of jump in velocity across the interface which is defined by:

$$\dot{\mathbf{w}}^{EE'} = \dot{\mathbf{w}}^{E'} - \dot{\mathbf{w}}^{E} \tag{6}$$

Equation (5) means that the value of the forces $\mathbf{f}^E(M,t)$ at time t depends of the history of the jump in velocity between time 0 and time t. If the behavior law must take into account the history of the jump in displacement (contact conditions with friction Coulomb's law), this value is computed using the integration scheme presented in Eq. (18).

In the simple case of a perfect connection between two substructures would be modeled by the following behavior:

$$\dot{\mathbf{w}}^{EE'}(M,t) = 0, \quad \forall M \in \Gamma^{EE'}, \forall t \in [0,T], \tag{7}$$

The form of the evolution law $\mathscr{R}$ in the case of frictional contact conditions is described in Sect. 2.5.

2.4 The LATIN algorithm

A LATIN (LArge Time INcrement) approach [1] is used to solve the problem. The solution s of the problem is written as a set of time-dependent fields on each substructure and related interfaces:

$$s = \sum_E s^E$$
$$s^E = \left\{\mathbf{u}^E(M,t), \sigma^E(M,t), \dot{\mathbf{w}}^E(M,t), \mathbf{f}^E(M,t)\right\}$$
$$t \in [0,T]$$

The LATIN approach is based on the idea of isolating the difficulties in order not to have to solve a global and nonlinear problem at the same time. The equations are split into two groups with the following two sets of solutions:

– the set $\mathscr{A}_d$ of solutions s^E to the linear equations related to the substructures (Eqs. 1–3)
– the set Γ of solutions s^E to the local equations (which may be nonlinear) related to the interfaces (Eqs. 4– 5)

The search for the overall solution (i.e., the intersection of the two sets) is conducted iteratively by constructing approximate solutions s which verify the two groups of equations alternatively on the complete time history. Thus, each iteration in the process is composed of two stages:

Local stage: for $s_n \in \mathscr{A}_d$ known, find $\widehat{s}$ such that:

$$\widehat{s} \in \Gamma \quad (interfaces) \tag{8}$$
$$\widehat{s} - s_n \in E^+ \quad (search\ direction) \tag{9}$$

Global stage: for $\widehat{s} \in \Gamma$ known, find s_{n+1} such that:

$$s_{n+1} \in \mathscr{A}_d \quad (substructures) \tag{10}$$
$$s_{n+1} - \widehat{s} \in E^- \quad (search\ direction) \tag{11}$$

The search directions E^+ and E^- are chosen such that the convergence of the algorithm is ensured [1]. These conjugate search directions depend on the scalar parameter k_0:

$$\widehat{s} - s_n \in E^+ \equiv (\widehat{\mathbf{f}}^E - \mathbf{f}^E_n) = k_0(\widehat{\mathbf{w}}^E - \dot{\mathbf{w}}^E_n) \tag{12}$$
$$s_{n+1} - \widehat{s} \in E^- \equiv (\mathbf{f}^E_{n+1} - \widehat{\mathbf{f}}^E) = -k_0(\dot{\mathbf{w}}^E_{n+1} - \widehat{\mathbf{w}}^E) \tag{13}$$

The solution of the problem does not depend on the value of the parameter k_0. It only affects the convergence rate of the algorithm. For quasistatic cases, which are studied here, k_0 is given by :

$$k_0 = \frac{E}{TL_c}$$

where E is the Young's modulus, $[0, T]$ is the studied time interval and L_c the largest dimension of the structure.

An error indicator is used to control the convergence of the algorithm. This indicator is an energy measure of the distance between the two solutions successive s_n and $\widehat{s}$.

In our particular case of linear elastic substructures, the inner solution (in displacement $\mathbf{u}^E(M,t)$ and in stress $\sigma^E(M,t)$) can easily be calculated from the boundary values ($\dot{\mathbf{w}}^E(M,t)$ and $\mathbf{f}^E(M,t)$). Therefore, from here on, a solution s will be represented only by the force and velocity fields on both sides of an interface.

2.5 The frictional contact interface

Contact problems are characterized by constraints such as nonpenetration conditions, and an active area of contact—that is, an area where contact effectively occurs—that is unknown a priori. For these reasons, these problems lead to stiff nonlinear systems of equations. Several approaches exist for solving static contact problems [8,9]. In most of them, the numerical methods that are employed for enforcing the contact constraints can be grouped into Lagrange multiplier and penalty methods. The penalty methods [10,11] are closely related to the regularization of the contact constraints. They are usually formulated in terms of the displacement variables, and therefore are primal methods. They allow treating contact as a material behavior, as examplified by the method of joint finite elements [12]. Penalty methods can experience various numerical difficulties, especially ill-conditioning, when a too

large or too small penalty parameter is introduced. Lagrange multiplier methods are dual methods where the multipliers, which represent the contact reaction forces, are introduced in order to enforce exactly the nonpenetration conditions. Augmented Lagrange multiplier methods [13–16] result in mixed formulations involving both displacement and force unknowns. The numerical solution schemes underlying both the Lagrange multiplier and augmented Lagrange multiplier methods are often related to the Uzawa algorithm [17–19].

The following sections describe the form of $\mathscr{R}$ evolution law in the case of frictional contact conditions.

2.5.1 The contact problem

The normal, oriented from Ω_E to $\Omega_{E'}$, at each point of an interface is designated by $\mathbf{i}$. The projection operator on the tangential plane P is defined by:

$$P\mathbf{w} = \mathbf{w} - (\mathbf{i}.\mathbf{w})\mathbf{i}$$

The nonpenetrating contact conditions are

- *Open*: if $\mathbf{i}.\widehat{\mathbf{w}}^{EE'} > 0$ then $\mathbf{i}.\widehat{\mathbf{f}}^{E} = \mathbf{i}.\widehat{\mathbf{f}}^{E'} = 0$.
- *Contact*: if $\mathbf{i}.\widehat{\mathbf{w}}^{EE'} = 0$ then $\mathbf{i}.\widehat{\mathbf{f}}^{E} = -\mathbf{i}.\widehat{\mathbf{f}}^{E'} \leq 0$.

These conditions can be written simply as

- *Open*: $c_i > 0$.
- *Contact*: $c_i \leq 0$.

where the contact indicator c_i is

$$c_i = \frac{1}{2T}\mathbf{i}.\widehat{\mathbf{w}}^{EE'} - \frac{1}{2k_0}\mathbf{i}.(\widehat{\mathbf{f}}^{E'} - \widehat{\mathbf{f}}^{E}) \tag{14}$$

2.5.2 The friction problem

Coulomb's friction conditions can be written as

- *Stick*: if $\|P\widehat{\mathbf{f}}^{E}\| < \mu|\mathbf{i}.\widehat{\mathbf{f}}^{E}|$ then $P\widehat{\mathbf{w}}^{EE'} = 0$.
- *Slip*: if $\|P\widehat{\mathbf{f}}^{E}\| = \mu|\mathbf{i}.\widehat{\mathbf{f}}^{E}|$ then $\exists\lambda > 0$ such that $P\widehat{\mathbf{w}}^{EE'} = -\lambda\widehat{\mathbf{f}}^{E}$.

These conditions can be written simply as

- *Stick*: $\|\mathbf{g}_j\| \geq \mu|\mathbf{i}.\widehat{\mathbf{f}}^{E}|$.
- *Slip*: $\|\mathbf{g}_j\| < \mu|\mathbf{i}.\widehat{\mathbf{f}}^{E}|$.

where the slip indicator $\mathbf{g}_j$ is

$$\mathbf{g}_j = \frac{k_0}{2}P\widehat{\mathbf{w}}^{EE'} - \frac{1}{2}P(\widehat{\mathbf{f}}^{E'} - \widehat{\mathbf{f}}^{E}) \tag{15}$$

2.5.3 Resolution

The resolution is carried out by projecting the solution of the previous global stage onto the contact and friction conditions following the search directions:

$$(\widehat{\mathbf{f}}^{E} - \mathbf{f}_n^{E}) = k_0(\widehat{\mathbf{w}}^{E} - \dot{\mathbf{w}}_n^{E}) \tag{16}$$

$$(\widehat{\mathbf{f}}^{E'} - \mathbf{f}_n^{E'}) = k_0(\widehat{\mathbf{w}}^{E'} - \dot{\mathbf{w}}_n^{E'}) \tag{17}$$

The status (*Open*, *Contact*, *Stick* or *Slip*) of each point of the interface is obtained explicitly since the indicators c_i and $\mathbf{g}_j$ can be derived from the previous solution using the search direction. An implicit time integration scheme is used to calculate the contact indicator c_i expressed in terms of the displacements (see Eq. 14):

$$\widehat{\mathbf{w}}_{(t+1)}^{EE'} = \widehat{\mathbf{w}}_{(t)}^{EE'} + \Delta t\,\widehat{\dot{\mathbf{w}}}_{(t+1)}^{EE'} \tag{18}$$

where $\mathbf{i}.\widehat{\mathbf{w}}_{(t=0)}^{EE'}$ is the initial gap and $P.\widehat{\mathbf{w}}_{(t=0)}^{EE'} = 0$. In order to use this integration scheme, the contact indicator is modified as

$$\tilde{c}_i = \frac{1}{2\Delta t}\mathbf{i}.\widehat{\mathbf{w}}^{EE'} - \frac{1}{2k_0}\mathbf{i}.(\widehat{\mathbf{f}}^{E'} - \widehat{\mathbf{f}}^{E}) \tag{19}$$

in order to obtain using the time integration (Eq. 18) and the search directions (Eqs. 16 and 17):

$$\begin{aligned}\tilde{c}_{i(t+1)} &= \frac{1}{2\Delta t}\mathbf{i}.\widehat{\mathbf{w}}_{(t+1)}^{EE'} - \frac{1}{2k_0}\mathbf{i}.(\widehat{\mathbf{f}}_{(t+1)}^{E'} - \widehat{\mathbf{f}}_{(t+1)}^{E}) \\ &= \frac{1}{2}\mathbf{i}.\widehat{\dot{\mathbf{w}}}_{(t+1)}^{EE'} - \frac{1}{2k_0}\mathbf{i}.(\widehat{\mathbf{f}}_{(t+1)}^{E'} - \widehat{\mathbf{f}}_{(t+1)}^{E}) + \frac{1}{2\Delta t}\mathbf{i}.\widehat{\mathbf{w}}_{(t)}^{EE'} \\ &= \frac{1}{2}\mathbf{i}.\dot{\mathbf{w}}_{n(t+1)}^{EE'} - \frac{1}{2k_0}\mathbf{i}.(\mathbf{f}_{n(t+1)}^{E'} - \mathbf{f}_{n(t+1)}^{E}) + \frac{1}{2\Delta t}\mathbf{i}.\widehat{\mathbf{w}}_{(t)}^{EE'}\end{aligned}$$

Thus, the contact indicator is calculated incrementally from the known solution to the previous global stage.

The slip indicator $\mathbf{g}_j$ (Eq. 15) is calculated explicitly using the search directions (Eqs. 16 and 17):

$$\mathbf{g}_j = \frac{k_0}{2}P\dot{\mathbf{w}}_n^{EE'} - \frac{1}{2}P(\mathbf{f}_n^{E'} - \mathbf{f}_n^{E}) \tag{20}$$

2.6 Discretization

Standard finite element discretization is used for the displacement field in the substructures:

$$\mathbf{u} = [N]\{u\} \quad \text{and} \quad \epsilon(\mathbf{u}) = [B]\{u\} \tag{21}$$

On the interfaces, a compatible discretization is applied to the velocity fields:

$$\widehat{\mathbf{w}}^{E} = [N]\{\widehat{w}^{E}\} \quad \text{and} \quad \dot{\mathbf{w}}_n^{E} = [N]\{\dot{w}_n^{E}\} \tag{22}$$

The search directions considered (Eqs. 13 and 13) lead one to choose the same discretization for the forces and for the velocity:

$$\widehat{\mathbf{f}}^{E} = [N]\{\widehat{f}^{E}\} \quad \text{and} \quad \mathbf{f}_n^{E} = [N]\{f_n^{E}\} \tag{23}$$

At the local stage, the contact equations are solved directly in terms of the nodal forces and velocities. Moreover, this representation of the forces (Eq. 23) plays a regularizing role for Coulomb's frictional problem: the friction law becomes thus non local [20,21].

2.7 Resolution for the global stage

At the global stage, the equilibrium equation (Eq. 2), which also takes into account kinematic admissibility (Eq. 1), the behavior (Eq. 3) and the search direction (Eq. 13), becomes:

$$\int_{\Omega_E} Tr(\epsilon(\mathbf{u}_n^E)\mathbf{D}\epsilon(\dot{\mathbf{u}}^\star))d\Omega_E = \int_{\partial\Omega_E} (\widehat{\mathbf{f}}^E - k_0(\dot{\mathbf{u}}_n^E - \widehat{\mathbf{w}}^E)).\dot{\mathbf{u}}^\star dS \tag{24}$$

$$\int_{\Omega_E} Tr(\epsilon(\mathbf{u}_n^E)\mathbf{D}\epsilon(\dot{\mathbf{u}}^\star))d\Omega_E + \int_{\partial\Omega_E} k_0\dot{\mathbf{u}}_n^E.\dot{\mathbf{u}}^\star dS = \int_{\partial\Omega_E} (\widehat{\mathbf{f}}^E + k_0\widehat{\mathbf{w}}^E).\dot{\mathbf{u}}^\star dS \tag{25}$$

After discretization, Eq. 25 becomes:

$$k_0\left[\mathbf{h}^E\right]\{\dot{u}(t)\} + [\mathbf{K}^E]\{u(t)\} = [\mathbf{h}^E]\left(\{\{\widehat{f}^E\}(t)\} + k_0\{\widehat{\dot{w}}^E\}(t)\right) \tag{26}$$

where

$$[\mathbf{h}^E] = \int_{\partial\Omega_E} [N]^t[N]ds \quad \text{and} \quad [\mathbf{K}^E] = \int_{\Omega_E} [\mathbf{B}]^t\,\mathbf{D}\,[\mathbf{B}]d\Omega$$

$[\mathbf{K}^E]$ is the classical finite element stiffness matrix of substructure Ω_E and $[\mathbf{h}^E]$ is the boundary term related to the interfaces.

For the resolution of the differential equation (Eq. 26), an Euler implicit time integration scheme is used. Then, the boundary terms are calculated at each time step:

$$\{\dot{w}_n^E\} = [\mathbf{R}]\{\dot{u}_n^E\} \tag{27}$$

where $[\mathbf{R}]$ is the restriction operator on $\partial\Omega_E$. The forces are obtained using the search direction:

$$\{f_n^E\} = \{\widehat{f}^E\} - k_0(\{\dot{w}_n^E\} - \{\widehat{\dot{w}}^E\}) \tag{28}$$

Finally, the algorithm can be summarized as shown in Table 1.

Table 1 Algorithm

Initialize
Loop on the substructures (E)
Compute $[K^E]$ and $[h^E]$.
Factorization.
Loop on the interfaces
$\{\dot{w}_0^E\} = \{\dot{w}_0^{E'}\} = \{\widehat{\dot{w}}^E\} = \{\widehat{\dot{w}}^{E'}\} = \{0\}$
$\{f_0^E\} = \{f_0^{E'}\} = \{\widehat{f}^E\} = \{\widehat{f}^{E'}\} = \{0\}$
Iterate $n = 1, 2, \ldots$ until convergence
Global stage : loop on the substructures (E)
Assemble the right hand side in Eq. 26
Integrate $\{\dot{u}(t)\}$ (Eq. 26)
Compute $\{\dot{w}_n^E\}$ (Eq. 27)
Compute $\{f_n^E\}$ (Eq. 28)
Local stage : loop on the interfaces (EE')
Compute c_i (Eq. 19)
Compute the normal part of $\{\widehat{\dot{w}}^E\}$, $\{\widehat{\dot{w}}^{E'}\}$, $\{\widehat{f}^E\}$ and $\{\widehat{f}^{E'}\}$ with respect to the sign of c_i.
Compute $\mathbf{g}_j$ (Eq. 20)
Compute the tangential part of $\{\widehat{\dot{w}}^E\}$, $\{\widehat{\dot{w}}^{E'}\}$, $\{\widehat{f}^E\}$ and $\{\widehat{f}^{E'}\}$ with respect to the value of $\|\mathbf{g}_j\|$.
Convergence test

2.8 Remarks

When only static cases and perfect connections are considered, this algorithm can be obtained by other approaches such as in Lions [22] or Glowinski and Le Tallec [23]. In the case of frictional contact static cases it is not very far from augmented lagrangian algorithms as presented by Simo and Laursen [18] or Zavarise and Wriggers [24].

As for augmented lagrangian algorithms, the number of iterations can be elevated. But here, as only elastic behavior of the substructures is considered, the operators $\mathbf{K}$ and $\mathbf{h}$ remain constant and independent of the iteration and of the contact status. Thus the cost of each iteration is low.

Moreover, it is very important to observe that the velocity and force fields on the interfaces constitute the only information needed for the subsequent iterations.

3 Strategy for multiple analysis

The strategy proposed consists in calculating response surfaces such that each point of a surface is associated with a

design configuration. Each design configuration corresponds to a set of values of all the variable parameters (friction coefficients, prestresses) which are introduced into the mechanical analysis.

At each iteration, the LATIN method leads to an approximate solution to the problem over the whole time interval. Therefore, the trick is to reuse this approximation (associated to one set of values of all the design parameters) to find the solution to another design configuration (another set of the design parameters) similar to the one for which it was calculated in the first place. Our strategy for multiple analysis uses the fact that the LATIN algorithm can be initialized with any solution (usually an elastic solution) provided that it verifies the admissibility conditions. Therefore, the key to our technique is to initialize the process associated with a new design configuration using the results of the calculation carried out on the first set of values of the design parameter. In this manner, a first approximation of the solution to the new design with a strong mechanical content is immediately available from the start.

In this particular case of elastic structures in contact, the interfaces play a vital role: they enable one to initiate the calculation on the new design configuration without having to save all data on the substructures as well as to search for the solution of the new design configuration with an initial solution well-suited to the target problem. In the best-case scenario, only a few iterations are necessary: the solution to the problem is obtained at low cost. If the solutions to the design configurations are close enough, the latter can still be derived at a significantly lower cost than by using a full calculation. For the parametric study presented herein, we just change the parameters between iterations. Thus, the new computation is initialized by the solution to the previous one. If the parameters change slowly, the two solutions are close and only a few iterations are needed to reach convergence in the new calculation.

4 First example: academic problem

Let us consider the simple example of a $40 \times 40 \times 40$mm cube subjected to frictional contact against a rigid body at Plane $z = 0$ (see Fig. 3). The material is elastic (Young's modulus $E = 130$ GPa, Poisson's ratio $\nu = 0.2$). Symmetry conditions are prescribed at Planes $x = 0$ and $y = 0$. The cube is pushed against the rigid body through the application of a pressure P1 = 5 MPa over its upper side. The remaining two sides are successively loaded and unloaded (P2 = 10 MPa and P3 = 10 MPa) in order to generate friction at the contact surface. The geometry and loading conditions are shown in Fig. 3.

The problem's only parameter is the friction coefficient, which was allowed to take 21 values (from 0 to 2 in increments of 0.1). We studied the quasi-static, small-perturbation problem.

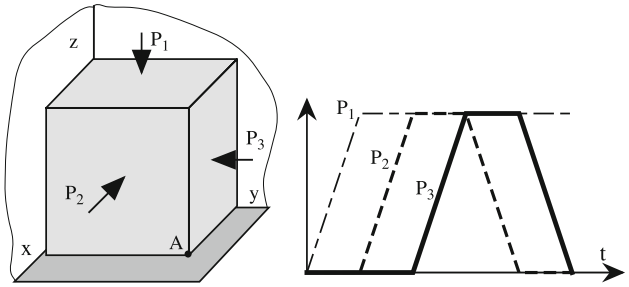

Fig. 3 Cube example: model and loading conditions

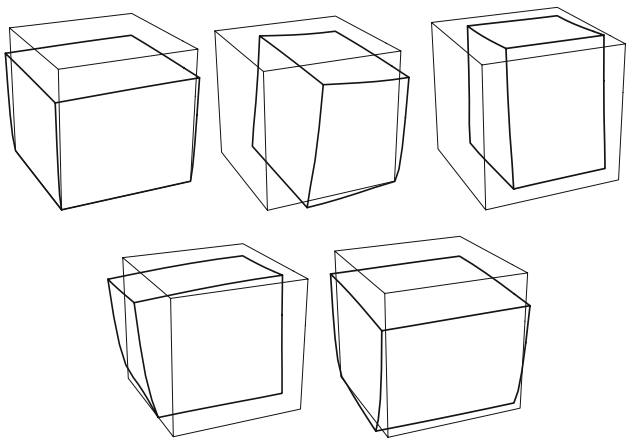

Fig. 4 Deformed shape

The mesh was composed of 100 eight-node brick elements (460 degrees of freedom). Figure 4 shows the deformed shape (magnified 400 times) of the cube with a friction coefficient equal to 0.4 after completion of five loading stages (application of P1, application of P2, application of P3, removal of P2 and, finally, removal of P3). Each stage was completed in 10 time steps. We studied the displacements of Point A (Fig. 4) in the contact plane ($z = 0$). Figure 5 shows the paths followed by Point A for the 21 values of the friction coefficient. Figure 6 shows the evolution of the error indicator, which increases at each change of the friction coefficient.

The computation cost was compared with that of a direct analysis using ABAQUS. Figure 7 shows the cost of each of the 21 calculations. One can observe that in the case of ABAQUS the computation cost increased with the friction coefficient. In the parametric study using the LATIN method, the computation cost decreased because the results of the successive computations, as shown by Fig. 6, were very close to one another. Thus, even though the first calculation cost three times as much as with the direct method, the total cost of the parametric study using the LATIN method was reduced by a factor of 1.5.

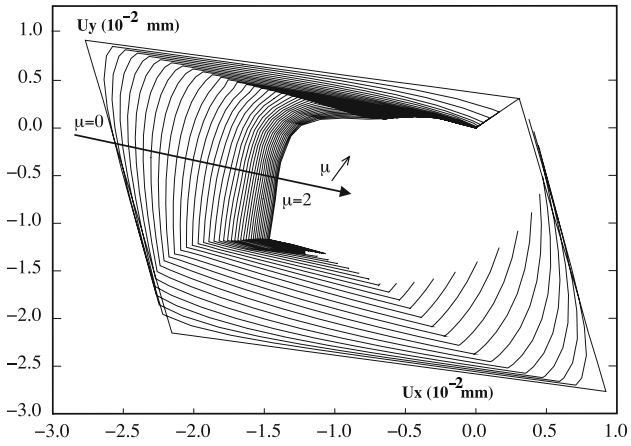

Fig. 5 Movement of point A

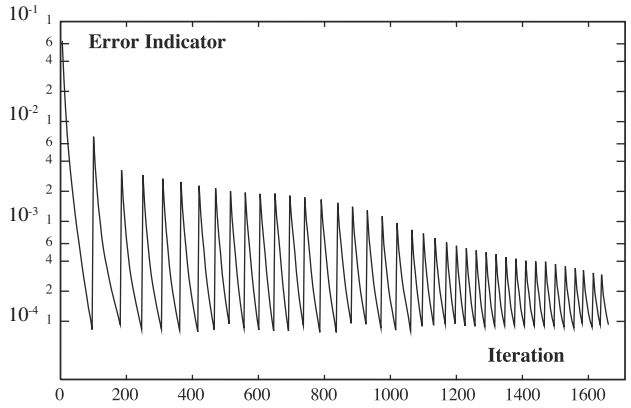

Fig. 6 Error indicator

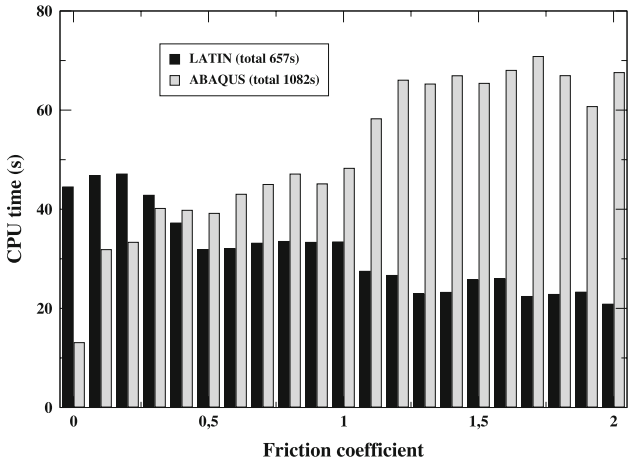

Fig. 7 Cost of each calculation

5 Application to a 3D assembly

Now, let us consider the example of an all-steel, zero-backlash disc coupling whose purpose is to compensate axial, radial and angular misalignments. This coupling transmits the torque, up to the maximum permissible impact torque,

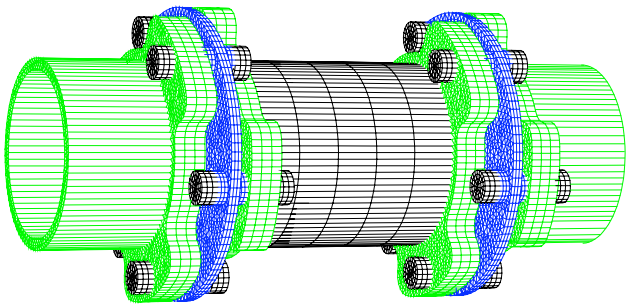

Fig. 8 FE mesh of the disc coupling

with a very high torsional stiffness. The materials are elastic (Young's modulus $E = 200$ GPa for all the materials except for the two thinner intermediate plates: Young's modulus $E = 70$ GPa; Poisson's ratio $\nu = 0.3$). Figure 8 shows the finite element mesh of the assembly. The decomposition into substructures of one-half of the assembly is shown in Fig. 9 (the same decomposition was used for the other half.)

The assembly was fixed at one end. The load consisted of a prestrain of the bolts followed by a 1° prescribed rotation at the other end. We considered the quasi-static, small-perturbation problem. The mesh was composed of 48,370 elements (130,250 degrees of freedom).

In the parametric study reported below, 11 values of the friction coefficient μ (from 0.05 to 0.55 in increments of 0.05) and 9 values of the prestrain p of the bolts (from 0.02 to 0.18 mm in increments of 0.02 mm) were considered. The quantity of interest was the evolution of the torsional moment as a function of the prescribed rotation (1°).

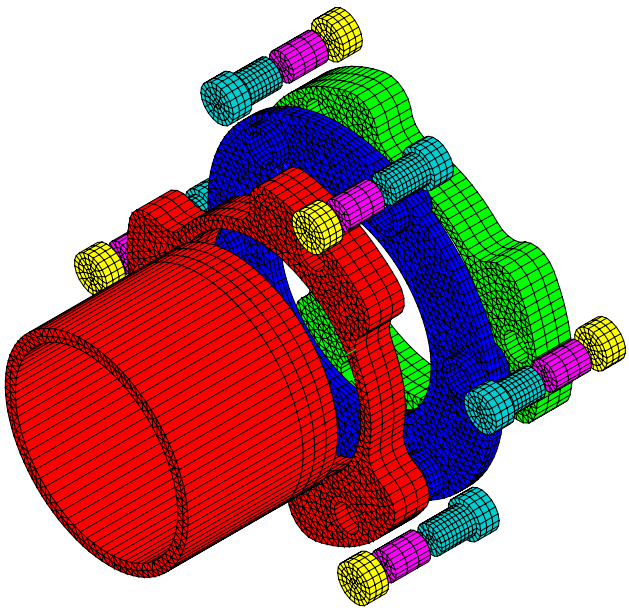

Fig. 9 Substructures used for the LATIN method

Table 2 Algorithm for the parametric study with the LATIN Method

Initialize
Loop on the substructures (E)
Compute $[K^E]$ and $[h^E]$ and factorize.
Loop on the interfaces
$\{\dot{w}_0^E\} = \{\dot{w}_0^{E'}\} = \{\widehat{\dot{w}}^E\} = \{\widehat{\dot{w}}^{E'}\} = \{0\}$
$\{f_0^E\} = \{f_0^{E'}\} = \{\widehat{f}^E\} = \{\widehat{f}^{E'}\} = \{0\}$
Define limits of parameter sets
Loop $k = 1, 2, \ldots$ number of parameter sets
Restore quantities on the interfaces
Iterate until convergence
Global stage : see Table 1
Local stage : see Table 1
Convergence test
Save interface solution for k^{th} parameter set

Following the same strategy as above, we carried out 99 different calculations (Table 2) in 9 groups of calculations at fixed value of p in which the value of μ was modified during the iterations.

Figure 10 shows the evolution of the torsional moment as a function of the prescribed rotation for $p = 0.16$ mm and

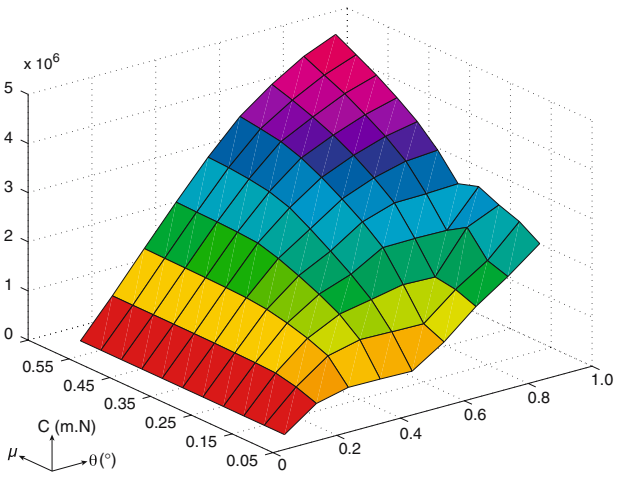

Fig. 10 Torsional moment versus prescribed rotation for $p = 0.16$ mm and for several values of μ

Table 3 Comparison of the costs of different calculation strategies

Calculation	Cost (s)	Cost (h)
Direct LATIN	451,440	125,7
Parametric LATIN (sequential)	130,500	36
Parametric LATIN (parallel)	14,500	4

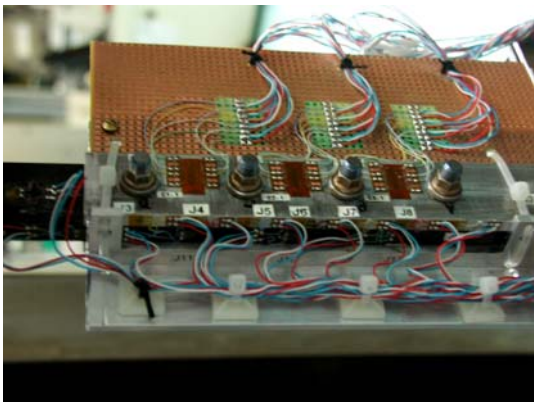

Fig. 11 Real tests carried out at EADS-IW

for different values of μ. Table 3 shows the comparison of the computation costs of the different strategies:

- all 99 calculations carried out on a single processor (direct LATIN).
- the 9 parametric calculations (one for each value of p) carried out sequentially on a single processor.
- the same 9 parametric calculations carried out concurrently on 9 processors.

6 Application to a bolted joint used in the aerospace industry

Let us now consider the example of a bolted joint. This example was derived from tests conducted at EADS-IW on four-bolt joints (see Fig. 11). These tests indicated that the life expectancy of such joints is sensitive to friction, pretension in the bolts, clearances, ... These parameters are naturally scattered, and a full test campaign to evaluate their actual influence would involve a very large number of specimens. This inspired EADS-IW to investigate a more cost-effective numerical approach in association with LMT Cachan.

The dimensions of the part of the connection being studied are shown in Fig. 12. The connection of the three plates is achieved through prestressed bolts. The upper and lower plates are made of aluminum (Young's modulus $E_a = 70$ GPa, Poisson's ratio $\nu_a = 0.3$). The intermediate plate is made of a carbon composite $[90, 45, 0, 135, 0, 45, 90, 135, 0, 0, 45, 0, 135, 0]_s$. The homogenized orthotropic mechanical characteristics of this material are $E_1 = 130$ GPa, $E_2 = E_3 = 4.65$ GPa, $\nu_{12} = \nu_{13} = \nu_{23} = 0.35$, $G_{12} = 10$ Gpa, $G_{13} = G_{23} = 4.65$ GPa (with directions 1,2,3 as defined in Fig. 12). The bolts are made of titanium (Young's modulus $E_t = 110$ GPa, Poisson's ratio $\nu_t = 0.3$).

The prestresses in the bolts are represented by relative displacements, denoted $Pre1$, $Pre2$, $Pre3$ and $Pre4$, between

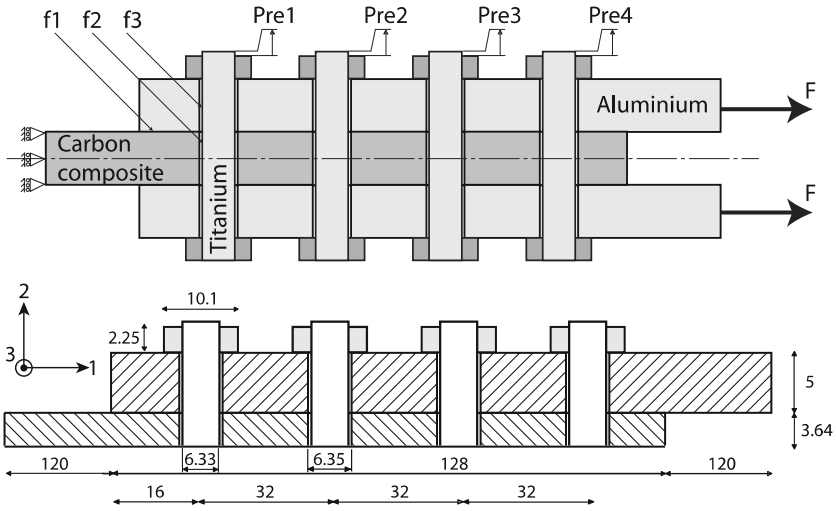

Fig. 12 Assembly configuration and dimensions (all in *mm*), thickness: 25.4 mm

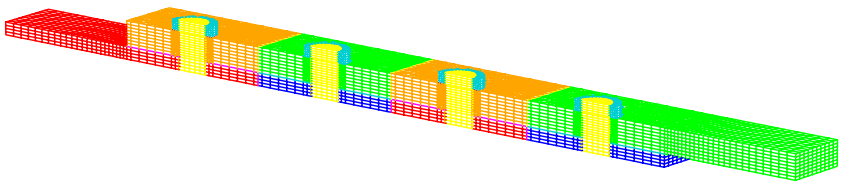

Fig. 13 Mesh of the bolted joint

the body and head of each bolt (Fig. 12). The friction coefficients are denoted $f1$ for aluminium/composite, $f2$ for titanium/composite and $f3$ for titanium/aluminium. In the parametric study, we analyzed the influence of the prestresses in the bolts and the friction coefficient on the forces transmitted by friction. In the first calculation, we evaluated the influence of the friction coefficient alone. Five values of each friction coefficient $f1$, $f2$ and $f3$ (from 0.05 to 0.45 in increments of 0.1) were considered. Thus, 125 computations had to be carried out. Then, we introduced the variations of the prestrains parameters. Five values of each prestrain $Pre1$, $Pre2$, $Pre3$ and $Pre4$ (from 0.1 to 0.18 in increments of 0.02) were considered, leading to 625 calculations.

The same mesh of the four bolts (31,792 linear tetrahedron or brick elements, 75,736 degrees of freedom) was used for all the calculations (Fig. 13). These were carried out in two steps:

- Step 1: prestress in the bolts,
- Step 2: traction on the specimen.

We studied the effects of the variability of the friction coefficients and the prestrains on the forces F_1, F_2, F_3 and F_4 which are the resultants of the friction forces around each bolts (see Fig. 14).

For example, Fig. 15 shows the evolution of the transmitted force F_1, for given values of the prestrains and two values of the friction coefficient f_1, as a function of the two other friction coefficients f_2 and f_3.

Figure. 16 summarizes all the results obtained for the variation of the four prestrains $Pre1$, $Pre2$, $Pre3$ and $Pre4$.

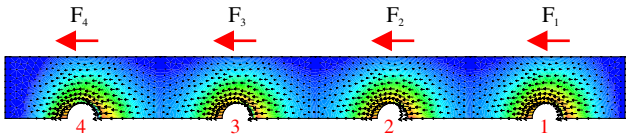

Fig. 14 Friction forces in the assembly

One can observe that the transmitted forces are highly sensitive to the friction coefficients and the prestrains.

Tables 4 and 5 show how the computation costs of the different strategies for each parametric analysis (125 calculations for the variation of the friction coefficients and 625 calculations for the variation of the prestrains) compare in terms of:

- the computation time for one computation;
- the different calculations carried out on a single processor (direct LATIN);
- the parametric strategy carried out on a single processor (Parametric LATIN).

This comparison shows that the global cost of the parametric study using the LATIN method was less by a factor ranging between 18 and 22.

7 Conclusion

We proposed a multi-analysis computational strategy based on the LATIN method, which takes advantage of its capability to reuse the solution of a problem in order to solve similar

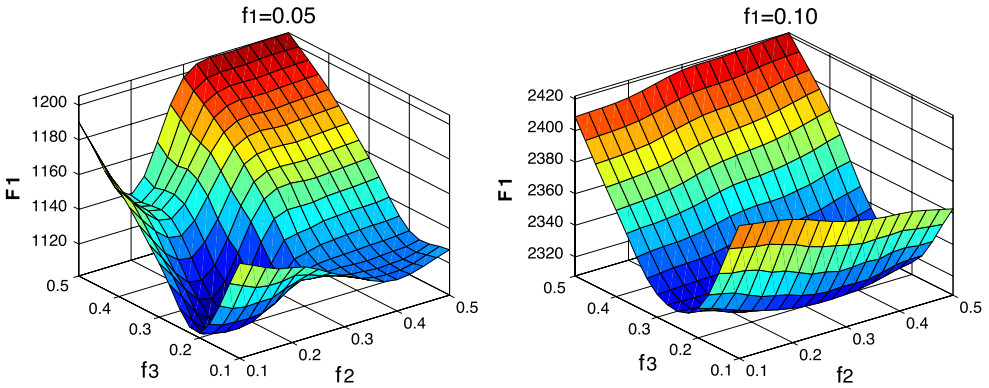

Fig. 15 Evolution of the transmitted forces F_1 (N) vs. the friction coefficients

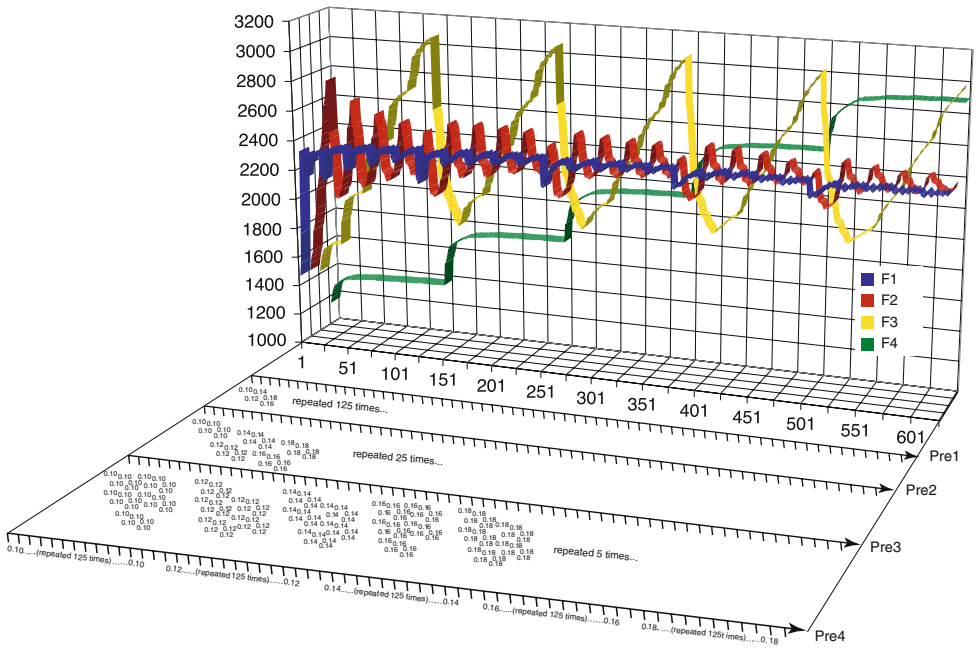

Fig. 16 Evolution of the transmitted forces F_1, F_2, F_3 and F_4 (N) versus the prestrains (mm)

Table 4 Cost comparison–variation of the friction coefficients

Calculation	Cost (CPU Time)
1 computation	32 mn
125 computations—direct LATIN	66 h
125 computations—parametric LATIN	3.5 h

Table 5 Cost comparison—variation of the prestrains

Calculation	Cost (CPU Time)
1 calculation	32 mn
625 calculations—Direct LATIN	334 h
625 calculations—Parametric LATIN	15 h

problems. The solution of the initial problem is a very good starting point to perform calculations on other problems, provided the new conditions do not perturb the response excessively.

In this paper, we present the application of this strategy to the analysis of assemblies of elastic structures taking into account contact and friction. For these assemblies, parametric studies has been carried out on the values of the connection parameters (friction coefficient, gaps, ...). We showed the important role played by the interfaces—which models the connections in the description of the assembly—in the drastic reduction of the computation costs.

The presented examples showed that the algorithm can be very efficient numerically. The last one concerned a real 3D junction developped by EADS-IW. The parametric analysis is performed 20 times faster than with a direct approach.

This approach is quite general in nature and should be applicable to a number of other nonlinear problems.

The continuation of this study, which is now in progress, consists in the comparison of our numerical results with those of experimental tests conducted at EADS-IW.

References

1. Ladevèze P (1999) Nonlinear computational structural mechanics–new approaches and non-incremental methods of calculation. Springer, Heidelberg
2. Rajashekhar M-R, Ellingwood B-R (1993) A new look at the response surface approach for reliability analysis. Struct Saf 12:205–220
3. Boucard P-A, Champaney L (2003) A suitable computational strategy for the parametric analysis of problems with multiple contact. Int J Numer Methods Eng 57:1259–1281
4. Allix O, Vidal P (2001) A new multi-solution approach suitable for structural identification problems. Comput Methods Appl Mech Eng 191:2727–2758
5. Benaroya H, Rehak M (1998) Finite element methods in probabilistic structural analysis: a selective review. Appl Mech Rev 41(5):201–213
6. Blanzé C, Champaney L, Védrine P (2000) Contact problems in the design of a superconducting quadrupole prototype. Eng Comput 17(2/3):136–153
7. Blanzé C, Champaney L, Cognard J-Y, Ladevèze P (1995) A modular approach to structure assembly computations. Application to contact problems. Eng Comput 13(1):15–32
8. Zhong Z, Mackerle J (1992) Static contact problems: a review. Eng Comput 9:3–37
9. Wriggers P (1995) Finite element algorithms for contact problems. Arch Comput Methods Eng 2:1–49
10. Kikuchi N (1982) Penalty/finite element approximations of a class of unilateral contact problems. In: Penalty method and finite element method. ASME, New York
11. Armero F, Petz E (1998) Formulation and analysis of conserving algorithms for dynamic contact/impact problems. Comput Methods Appl Mech Eng 158:269–300
12. Alart P, Curnier A (1991) A mixed formulation for frictional contact problems prone to Newton like solution methods. Comput Methods Appl Mech Eng 92:253–375
13. Arora J-S, Chahande A-I, Paeng J-K (1991) Multiplier methods for engineering optimization. Int J Numer Methods Eng 32:1485–1525
14. Klarbring A (1992) Mathematical programming and augmented lagrangian methods for frictional contact problems. In: Curnier A (ed) Proceedings of the Contact Mechanics International Symposium, Presses Polytechniques et Universitaires Romandes, pp 409–422
15. Radi B, Baba O-A, Gelin J-C (1998) Treatment of the frictional contact via a Lagrangian formulation. In: Rodin E-Y, Shillor M (eds) Mathematical and Computer Modelling, vol 28. Pergamon Press, Oxford, pp 407–412
16. Chabrand P, Dubois F, Raous M (1998) Various numerical methods for solving unilateral contact problems with friction. In: Rodin E-Y, Shillor M (eds) Mathematical and Computer Modelling, vol 28. Pergamon Press, Oxford, pp 97–108
17. Arrow K-J, Hurwicz L, Uzawa H (1998) Studies in nonlinear programming. University Press, Stanford
18. Simo J-C, Laursen T-A (1992) An augmented lagrangian treatment of contact problems involving friction. Comput Struct 42:97–116
19. Champaney L, Cognard J-Y, Ladevze P (1999) Modular analysis of assemblages of three-dimensional structures with unilateral contact conditions. Comput Struct 73:249–266
20. Cocu M, Pratt E, Raous M (1996) Formulation and approximation of quasistatic frictional contact. Int J Eng Sci 34:783–798
21. Hild P (2002) On finite element uniqueness studies for Coulomb's frictional contact model. Int J Appl Math Comput Sci 12:41–50
22. Lions P-L (1990) On the Schwartz alternating method III: a variant for non-overlapping subdomains. In: Chan T, Glowinski R, Périaux J, Windlun O (eds) Proceedings of the 3rd Domain Decomposition Methods for Partial Differential Equations. SIAM, Philadelphia, pp 202–223
23. Glowinski R, Le Tallec P (1990) Augmented lagrangian interpretation of the non-overlapping Schwarz alternating method. In: Glowinski R, Périaux J, Widlund O-B (eds) Proceedings of the 3rd Conference on Domain Decomposition Methods, SIAM, Philadelphia, pp 224–231
24. Zavarise G, Wriggers P (1999) A super linear convergent augmented lagragian procedure for contact problems. Eng Comput 16(1):88–119